Article

Grinding Method for Phase Transformation of Glycine

Jeongki Kang,[#] Jinsoo Kim,[#] and Woo-Sik Kim*

Read Online

ACCESS | 📊 Metrics & More | 📄 Article Recommendations | 🆘 Supporting Information

ABSTRACT: Glycine had three polymorphs, two metastable phases (α-glycine, β-glycine) and one stable phase (γ-glycine). However, the phase transformation of glycine from α-phase to γ-phase was well known as the kinetically unfavorable process. In this study, a simple and effective grinding method for phase transformation of glycine from α-phase to γ-phase is proposed. In an aqueous solution, α-glycine and γ-glycine had bulk solubilities of 180 and ~172 g/L, respectively. According to the Ostwald−Freundlich equation, however, as the crystal size of α-glycine was reduced to ~0.6 μm by grinding, the saturated concentration of α-glycine increased from 180 to 191 g/L. As long as the solution concentration exceeds a critical point ($\sigma = 0.1$), it can be possible to suddenly induce the nucleation of γ-glycine by grinding the α-glycine crystal in the solution. Subsequently, the complete transformation of α-phase to γ-phase was achieved without additives. Similarly, the grinding method was effective for producing the γ-glycine crystal in the cooling crystallization whereas the α-glycine crystal was always produced in the cooling crystallization without grinding. This study showed that physical grinding can effectively facilitate phase transformation by triggering the nucleation of stable polymorph.
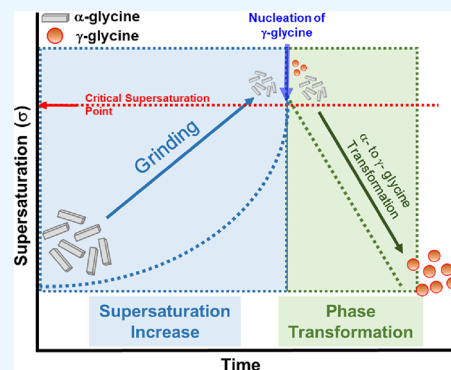
1. INTRODUCTION

Polymorphic control of active pharmaceutical ingredients (APIs) is essential for the pharmaceutical industry because polymorphs can affect the efficacy of drugs by changing pharmacokinetic and bioavailability derived from different physicochemical properties of polymorphs such as solubility, hygroscopicity, melting point, stability against various environmental factors (e.g., light, temperature, and humidity), and compressibility.[1−7] The most stable polymorph is typically selected over metastable forms since a phase transformation for metastable forms can alter a drug's pharmacokinetics and bioavailability.[8−10] In practice, the authorization or approval of a drug is occasionally revoked when the polymorphic form of APIs is transformed, resulting in the change of the pharmacokinetic and/or bioavailability characteristics during the manufacturing process, storage, and distribution.[8,9] For instance, Abbott Laboratories developed ritonavir in 1992, applied for a new drug application in 1995, released it on the market in January 1996, and received FDA approval in March 1996. At that time, ritonavir was sold in gelatin capsules (semi-solid capsules) or liquid form (oral liquid) with the trade name Novir.[7,11−13] However, several gelatin capsules did not meet the dissolution specifications because some gelatin capsules had been transformed into more stable polymorphs. As a result, the gelatin capsules were temporarily withdrawn from the market.[11] Therefore, a stable form that can well retain the physicochemical properties concerning pharmacokinetics and/or bioavailability over the metastable form has been preferred in the pharmaceutical industry.[11,14,15]

However, some API polymorphs (e.g., ritonavir, L-histidine, glycine) are easy to synthesize in their metastable form whereas the stable form is not easy to synthesize.[3,8] Thus, an additional process is required to transform the metastable form into the stable form.[8] Traditionally, glycine, the simplest amino acid having three kinds of polymorphs (α-, β-, and γ-glycine), is used as a model API in the pharmaceutical industry for polymorphic study.[16] Among polymorphs, α-glycine, a metastable form, is known to be readily nucleated and grew from a pure aqueous glycine solution, whereas γ-glycine, the most stable form, is slowly nucleated and grows only when adding additives such as acids, bases, and inorganic salts (i.e., L-malic acid, lauric acid, L-leucine, sodium chloride, and sodium nitrate).[16−22,27] Here, manufacturing costs and impurities can increase if additives were added during the glycine crystallization.[16−18] This study is an attempt to produce γ-glycine without adding additives.

The crystal's size affects its solubility in a solution. According to the Ostwald−Freundlich equation, the solubility of crystals is increased as the size of the crystal is decreased because the chemical potential of the molecules in the crystals is increased.[23,24] Correspondingly, it can be inferred that the

size reduction of α-glycine crystals can increase the solubility of α-glycine. Meanwhile, it can also be said that the supersaturation is increased as the solubility of α-glycine is increased to the perspective of γ-glycine. Eventually, when the solubility of α-glycine is continuously increased so that the supersaturation to the perspective of γ-glycine reaches a point called critical supersaturation, the nucleation of γ-glycine can occur. Accordingly, in this study, the nucleation and growth of γ-glycine were induced by reducing the size of α-glycine crystals using physical grinding methods (i.e., glass bead grinding and magnetic bar grinding). To the best of our knowledge, this is the first report of physical grinding-assisted phase transformation of glycine via a simple methodology at a constant temperature. This study will then argue that by increasing supersaturation to the critical supersaturation level, physical grinding can be employed to phase transition polymorphs from metastable to stable forms.

2. MATERIALS AND METHODS

2.1. Materials. γ-Glycine (glycine, 99.0%) was purchased from Samchun Co., and the structure of glycine was determined using X-ray diffraction (XRD, MiniFlex 600, Rigaku). Anhydrous ethyl alcohol (denatured, 99.5%) was bought from Daejung Co. The chemicals were used without further purification. α-Glycine was prepared by recrystallization of glycine as follows. At 50 °C for 1 h, 320 g of γ-glycine was completely dissolved in 1000 mL of deionized water. Then, the glycine solution was cooled down to 5 °C at a cooling rate of 45 °C/h and kept for 2 h for complete crystallization. The produced crystals were filtered with filter paper (No. 53, 1–2 μm, Hyundai Micro Munktel, South Korea) and dried at 60 °C in a forced convection oven (JEIO Tech, OF-12GW) for 6 h. Finally, 230 g of α-glycine (yield = 71.8%) was obtained and the crystal phase was confirmed with XRD. Here, the pure α-phase of the glycine crystal was obtained.[25,26]

2.2. Calibration of ATR-FTIR. In this study, the glycine concentration in solution was measured in real time using ATR-FTIR (ReactIR 15, DiComp probe with AgX halide fiber, Mettler-Toledo), as shown in Figure 1. First, ATR-FTIR was calibrated with the standard solution of glycine (2.176–198 g/L). Then, using the characteristic peak of glycine (1413 cm^{-1},

ν_s COO absorption), the standard calibration curve was plotted using the partial least square (PLS) regression method, as shown in Figure S1 (Supporting Information).

2.3. Determination of Solubility. Glycine crystals of each phase were ground using a mortar and then sieved to classify crystals in size (group 2–group 6). The crystals of group 2 were ground further using an air jet mill (2 open Manifold Micronizer, GNG Korea) and then sieved to obtain smaller crystals (group 1). Then, the crystal sizes of each group (group 1–group 6) were measured using a particle size analyzer (Malvern, Mastersizer 3000 with HYDRO-R and HYDRO EV), as shown in Table S1 (Supporting Information). Furthermore, the typical SEM images of α-glycine and γ-glycine in each group are shown in Figure S2 (Supporting Information).

The solubility of α-glycine and γ-glycine in each group was measured using in situ ATR-FTIR. An excess amount (54 g) of glycine crystal was added to 270 mL of deionized water at 10 °C and stirred with an impeller. The glycine concentration change in the solution was monitored by ATR-FTIR until the solution was saturated. The undissolved crystals were filtered and dried in a vacuum oven at room temperature for 2 h for XRD analysis (XRD, MiniFlex 600, Rigaku). The solubility of the crystal less than 5 μm was determined by the wet grinding method. As such, an excess amount (54 g) of glycine crystals in group 1 was added to 270 mL of deionized water at 10 °C in 300 mL of glass beaker with 200 g of glass beads (1.7–2.0 mm) and then ground by glass beads using impeller agitation, as shown in Figure 1.

Then, the agitation of the glass beads was stopped to sample the suspension at a specific time (550, 1250, and 2700 min). The sample was taken in the supernatant suspension of the crystallizer. The crystal size of the sample suspension was determined using a Zetasizer analyzer (Malvern Zetasizer Nano-ZS ZEN 3600). Simultaneously, the saturated concentration of glycine was measured with in situ ATR-FTIR. The structure of residual crystals was checked with XRD.

2.4. Experiment Setup. *2.4.1. Grinding for Phase Transformation.* Figure 1 shows that phase transformation of α-glycine to γ-glycine was conducted in a 300 mL mixing tank (MT) crystallizer. In the case of glass bead grinding, 54 g of α-glycine crystal in group 1 and 200 g of glass bead were added in the MT crystallizer filled with 270 mL of deionized water at 10 °C. Then, the glass beads were stirred with the impeller (propeller type impeller with a diameter 4 cm, four blades) at 200 rpm to grind the crystals. In the case of magnetic bar grinding, the experiment was conducted under the same conditions as those in the above experiment, such as the amount of α-glycine crystals in group 1 and water and temperature. However, in this experiment, the glass bead and impeller were not used. Instead, a magnetic bar was used to grind crystals at a rotation speed of 200 rpm. For the comparison with the above two grinding methods, the experiment was operated at the same conditions as those in the above two experiments except for the glass bead and magnetic bar. Therefore, the crystals in the crystallizer were agitated with an impeller without glass beads.

The glycine concentration in the solution was continuously monitored during the experiment using in situ ATR-FTIR. The sample suspension was intermittently taken for analysis of the crystal structure using XRD.

2.4.2. Grinding for Cooling Crystallization. For cooling crystallization of glycine, 270 mL of glycine solution (200 g/L)
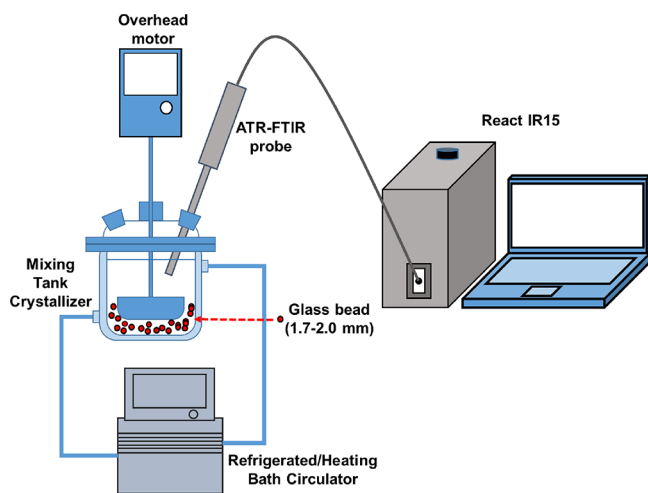
Figure 1. Schematic of the experimental setup of a batch cooling crystallization system consisting of an ATR FT-IR probe in a mixing tank (MT) crystallizer.
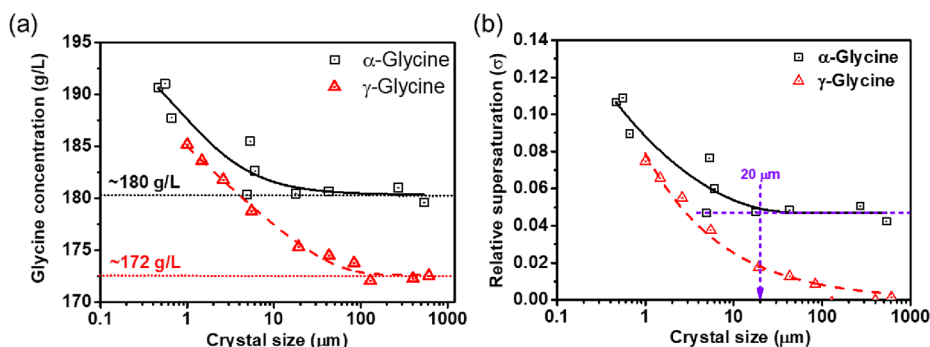
Figure 2. (a) Glycine concentration and (b) relative supersaturation of α- and γ-glycine depending on crystal size at 10 °C.
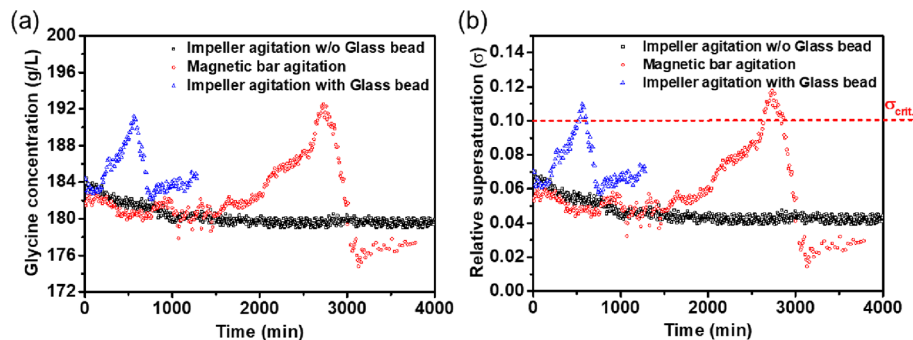
Figure 3. Effect of grinding (impeller agitation w/o glass beads, magnetic bar agitation, and impeller agitation with glass beads). (a) Glycine concentration (g/L) and (b) relative supersaturation (σ) profiles of glycine over time.

was added with 200 g of glass beads into the MT crystallizer at 50 °C. After 60 min, the crystallizer was cooled from 50 to 10 °C at a constant cooling rate of 10 °C/h. The glycine solution and then suspension, including the glass beads, were agitated with an impeller at 200 rpm for grinding the crystals. A sample was taken at 800, 1900, and 2400 min and then filtered and dried in a vacuum oven for XRD analysis during the cooling crystallization. The cooling crystallization was performed under the same conditions as the above experiment, except for the glass bead. Here, a sample was taken at 800 and 2400 min for XRD analysis of crystals.

3. RESULTS AND DISCUSSION

3.1. Effect of Crystal Size on Solubility. Figure 2a shows the effect of crystal size on solubility of α- and γ-glycine at 10 °C. Overall, α-glycine has higher solubility than γ-glycine because the chemical potential of metastable α-glycine was higher than that of stable γ-glycine. According to the Ostwald–Freundlich equation, the solubility of both α- and γ-glycine was increased as the crystal size was decreased because the chemical potential of the crystal was increased as the crystal size was decreased.[28,29] Here, the solubility of α-glycine was almost invariant at ~180 g/L for the crystal size over 20 μm (referred to as bulk solubility of α-glycine), whereas that of γ-glycine was approached to ~172 g/L for the crystal size over 130 μm (referring to bulk solubility of γ-glycine).

In the literature, solubility data of α-glycine and γ-glycine in water were reported. Yang et al.[31] and Igarashi et al.[32] showed solubility at 10 °C, and it was found to be consistent with our bulk solubility data mentioned earlier.

Figure 2b shows the effect of crystal size on the relative supersaturation of glycine, which is defined as

$$\sigma = (C_{eq}(r)_{glycine} - C_{eq}(\infty)_{\gamma-glycine})/C_{eq}(\infty)_{\gamma-glycine} \quad (1)$$

where $C_{eq}(r)_{glycine}$ is the saturated concentration of glycine at a crystal size of r (μm) and $C_{eq}(\infty)_{\gamma-glycine}$ is the bulk solubility of γ-glycine at an infinite size.[30] Here, bulk solubility of γ-glycine ($C_{eq}(\infty)_{\gamma-glycine}$ = 172 g/L) was used as a reference value to determine the relative supersaturation for nucleation of γ-glycine. The relative supersaturation of glycine was significantly increased up to 0.11 when the α-glycine crystal size was reduced to 600 nm whereas the relative supersaturation was merely increased up to 0.07 when the γ-glycine crystal size was decreased to around 1 μm. Thus, it can be inferred that increasing the saturated concentration of α-glycine according to the reduction of crystal size would provide a higher driving force for the induction of γ-glycine nucleation. In this sense, in the next section, a phase transformation study of α-glycine to γ-glycine was conducted by a grinding method at a consistent temperature (10 °C).

3.2. Effect of Grinding on Phase Transformation. As shown in Figure 3, the effect of grinding α-glycine crystal on the phase transformation was investigated. Here, glycine crystal in saturated solution was ground using the α-two kinds of methods: (1) glass bead grinding using an impeller stirrer and (2) magnetic bar grinding using a magnetic stirrer. In method (1), the crystal was ground by the attrition between glass beads, whereas in method (2), the crystal was ground by the abrasion between the magnetic bar and the bottom of the reactor. Furthermore, comparing the grinding effect, the α-glycine crystal was agitated by an impeller without a glass bead. Therefore, the glycine concentration in the solution was gradually increased as the α-glycine crystal was ground.

This solution was in a saturated state with the α-glycine crystal but was in a supersaturated state for γ-glycine, as expressed in terms of relative supersaturation (σ) in Figure 2b.

When this relative supersaturation of the solution exceeded the critical point ($\sigma_{crit.}$), rapid nucleation was triggered.[28,29] Thus, the sharp drop in solution concentration occurred after it reached ~192 g/L (relative supersaturation of ~0.11) for sudden nucleation of the γ-glycine crystal. Then, the γ-glycine crystal was continuously grown in the supersaturated solution until the α-glycine crystal was entirely dissolved out for phase transformation. Since the glass bead grinding was much more efficient for the crystal size reduction than magnetic bar grinding, the peak solution concentration in method (1) occurred much earlier than that in method (2). However, the peak solution concentration in method (2) was slightly higher than that in method (2) due to the slow reduction of crystal size. Here, note that even though the α-glycine crystal was completely transformed to γ-glycine crystal, the solution concentration did not approach the bulk solubility of γ-glycine ($\sigma = 0$) due to the grinding effect on the γ-glycine crystal. The γ-glycine crystal was also ground during the phase transformation, increasing the saturated concentration of the γ-glycine crystal in the solution. Thus, the relative supersaturation (σ) was always higher than zero and rather increased after reaching the minimum level of the relative supersaturation. In addition, due to the effectiveness of the grinding method, the minimum level of the relative superstation in glass bead grinding occurred much earlier. It was higher than that in magnetic bar grinding.

In contrast, when the α-glycine crystal was agitated by the impeller without a glass bead, the glycine concentration in the solution was never increased because of the absence of grinding (or attrition). Rather, the glycine concentration was slightly decreased due to the Ostwald ripening effect. Then, the glycine concentration slowly approached the bulk solubility of the α-glycine crystal, at 180 g/L.

The phase transformation of glycine crystal was confirmed by XRD, as shown in Figure 4. XRD patterns revealed that the
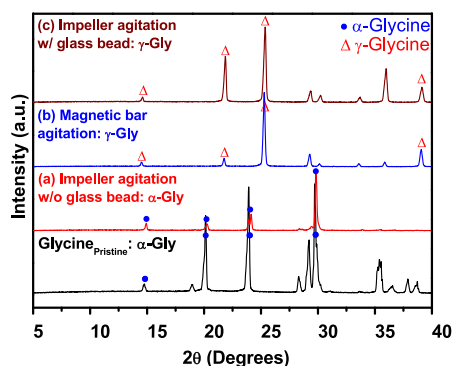
Figure 4. Crystal structure changes over time determined by X-ray diffraction. (a) Impeller agitation w/o glass beads, (b) magnetic bar agitation, and (c) impeller agitation w/ a glass beads.

α-glycine crystal was entirely converted to γ-glycine crystal when using the grinding method. However, in the case of impeller agitation without glass beads, the crystal structure of glycine remained as α-phase even after 4000 min. Therefore, it would be inferred from the above results that the grinding of the glycine for crystal size reduction was most critical and effective for phase transformation.

3.3. Effect of Grinding on Cooling Crystallization. Based on Ostwald's Rule of Stages, it was well known that the α-phase crystal was first formed in the crystallization of glycine

but hardly transformed to γ-phase without the additives.[18] In the present study, thus, the glass bead grinding method was applied for the promotion of phase transformation in the cooling crystallization of glycine. The clear glycine solution was cooled from 50 to 10 °C at a constant cooling rate of 10 °C/h for cooling crystallization. When the crystallization was agitated by an impeller without a glass bead, the solution concentration was sharply dropped after the induction of nucleation and gradually approached the saturated bulk concentration of the α-glycine crystal (~180 g/L), as shown in Figure 5b.

This result suggested that the α-phase of the crystal was first generated by the nucleation and approached the bulk equilibrium state with α-phase without any conversion to γ-phase even over 2500 min. However, two rapid drops of the solution concentration were observed when the crystallization was agitated with a glass bead, as shown in Figure 5c. The first drop of the solution concentration occurred at around ~200 min due to the nucleation of α-phase glycine. Then, the second drop of the solution concentration followed the first one around 1800 min later due to the nucleation of γ-phase glycine. Here, it would be interesting to find that the solution concentration in the interval between the first and second drops (between two nucleations of α- and γ-phase glycine) seemed to level off at around 188−190 g/L. This level was higher than the bulk saturated concentration of α-phase glycine (180 g/L) due to the glass bead grinding. That is, the solubility of α-phase glycine was increased by the crystal size reduction, as mentioned early. Precisely, the glass bead grinding slightly increased the solution concentration in this interval, exceeding the critical relative supersaturation ($\sigma_{crit.}$), as shown in Figure 5c. Therefore, it resulted in the second nucleation for γ-phase at around 2000 min. After then, the solution concentration was decreased due to the phase transformation of α-glycine crystal to γ-glycine crystal. Even though the phase transformation was completed at around 2200 min, the solution concentration was still higher than the saturated bulk concentration of the γ-glycine crystal (172 g/L) due to the grinding effect.

The glycine crystal was sampled during the crystallization for XRD analysis to confirm the phase transformation. The sample was taken at 800 min (A) and 2400 min (B) in the case of crystallization without glass bead grinding. In the crystallization with glass bead grinding, the glycine crystal was sampled at 800 min (C), 1900 min (D), and 2400 (E), as marked in Figure 5b,c. The crystal structure of the glycine obtained after the nucleation in the crystallizer without glass bead grinding was always of α-phase, as shown in Figure 6a.

Meanwhile, when the glass bead grind was used in the crystallization, it was discovered that the γ-glycine crystal was finally obtained at 2400 min after the second nucleation even though the α-glycine crystal was generated at the first nucleation. Therefore, it can be insisted that the phase transformation, which was a kinetically unfavorable process for glycine, was significantly facilitated by the grinding method for crystal size reduction.

4. CONCLUSIONS

It was successfully shown that glycine may be transformed by simple physical grinding. The grinding of the α-glycine crystal triggered the nucleation of γ-phase to facilitate the phase transformation of glycine from α-phase to γ-phase. According to the mechanism of the grinding method, as the crystal size was reduced to ~0.6 μm by the grinding, the saturated
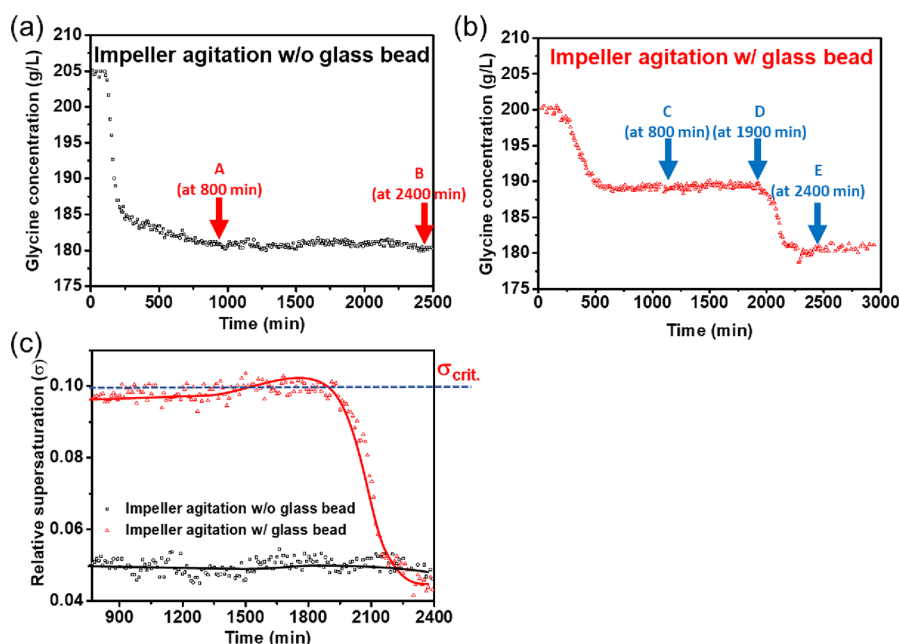
Figure 5. Effect of grinding. (a) Glycine concentration profile of impeller agitation w/o glass beads, (b) glycine concentration profile of impeller agitation with glass beads, and (c) relative supersaturation (σ) profile over time. Note: samples were collected at A, B, C, D, and E points and used for determining the crystal structure by X-ray diffraction.
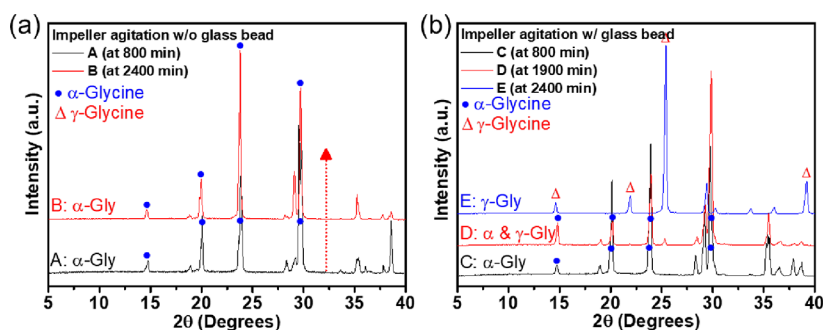
Figure 6. Crystal structure changes over time determined by X-ray diffraction. (a) Impeller agitation w/o glass beads at 800 and 2400 min and (b) impeller agitation with glass beads at 800, 1900, and 2400 min.

concentration of α-glycine was significantly increased from 180 to 191 g/L. The elevated solution concentration provided a high driving force to induct the nucleation of γ-phase, initiating the phase transformation of the α-glycine crystal to the γ-glycine crystal without any additive. Due to a more efficient reduction of crystal size, the glass bead grinding method was much better for the phase transformation of glycine than the magnetic bar grinding method. Similarly, the grinding method was critical in producing γ-glycine crystal in the cooling crystallization without any additive. However, only the α-glycine crystal was available in the crystallization without grinding. As a result, the grinding method was easily adaptable to facilitate kinetically unfavorable phase transformation of polymorphs.

■ ASSOCIATED CONTENT

ⓢ Supporting Information

The Supporting Information is available free of charge at https://pubs.acs.org/doi/10.1021/acsomega.3c01435.

ATR-FTIR spectra and calibration curve of glycine (Figure S1), SEM images of powder groups (Figure S2),

and particle size of the glycine powder group (Table S1) (PDF)

■ AUTHOR INFORMATION

Corresponding Author

Woo-Sik Kim − *Functional Crystallization Center, Department of Chemical Engineering (Integrated Engineering Program), Kyung Hee University, Yong-in, Gyeonggi-do 17104, South Korea;* ⓞ orcid.org/0000-0001-6876-4726; Phone: +82 031 201 2576; Email: wskim@khu.ac.kr; Fax: +82 031 2731 2970

Authors

Jeongki Kang − *Functional Crystallization Center, Department of Chemical Engineering (Integrated Engineering Program), Kyung Hee University, Yong-in, Gyeonggi-do 17104, South Korea; Process Research Department, Research & Development Division, Yuhan Corporation, Yong-in, Gyeonggi-do 17084, South Korea*

Jinsoo Kim − *Functional Crystallization Center, Department of Chemical Engineering (Integrated Engineering Program),*

Kyung Hee University, Yong-in, Gyeonggi-do 17104, South Korea

Complete contact information is available at:
https://pubs.acs.org/10.1021/acsomega.3c01435

Author Contributions

#J.Ka. and J.Ki. contributed to this work equally and should be regarded as co-first authors.

Author Contributions

All authors reviewed and agreed for the publication of this article.

Notes

The authors declare no competing financial interest.

■ REFERENCES

(1) Lu, J.; Rohani, S. Polymorphism and crystallization of active pharmaceutical ingredients (APIs). *Curr. Med. Chem.* **2009**, *16*, 884–905.

(2) Onoue, S.; Kojo, Y.; Aoki, Y.; Kawabata, Y.; Yamauchi, Y.; Yamada, S. Physicochemical and pharmacokinetic characterization of amorphous solid dispersion of tranilast with enhanced solubility in gastric fluid and improved oral bioavailability. *Drug Metab. Pharmacokinet.* **2012**, *27*, 379–387.

(3) Censi, R.; Di Martino, P. Polymorph impact on the bioavailability and stability of poorly soluble drugs. *Molecules* **2015**, *20*, 18759–18776.

(4) Zhou, Y.; Wang, J.; Xiao, Y.; Wang, T.; Huang, X. The effects of polymorphism on physicochemical properties and pharmacodynamics of solid drugs. *Curr. Pharm. Des.* **2018**, *24*, 2375–2382.

(5) Bauer, J. F. Polymorphism - A critical consideration in pharmaceutical development, manufacturing, and stability. *J. Valid. Technol.* **2008**, *14*, 15–24.

(6) Mannhold, R.; Buschmann, H.; Holenz, J. *Innovative Dosage Forms: Design and Development at Early Stage*; John Wiley & Son 2019.

(7) Wang, C.; Rosbottom, I.; Turner, T. D.; Laing, S.; Maloney, A. G. P.; Sheikh, A. Y.; Yin, Q.; Roberts, K. J. Molecular, solid-state and surface structures of the conformational polymorphic forms of ritonavir in relation to their physicochemical properties. *Pharm. Res.* **2021**, *38*, 971–990.

(8) Newman, A.; Wenslow, R. Solid form changes during drug development: good, bad, and ugly case studies. *AAPS Open* **2016**, *2*, 1–11.

(9) Zhang, G. G.; Law, D.; Schmitt, E. A.; Qiu, Y. Phase transformation considerations during process development and manufacture of solid oral dosage forms. *Adv. Drug Delivery Rev.* **2004**, *56*, 371–390.

(10) Purohit, H. S.; Taylor, L. S. Phase behavior of ritonavir amorphous solid dispersions during hydration and dissolution. *Pharm. Res.* **2017**, *34*, 2842–2861.

(11) Bauer, J.; Spanton, S.; Henry, R.; Quick, J.; Dziki, W.; Porter, W.; Morris, J. Ritonavir: An extraordinary example of conformational polymorphism. *Pharm. Res.* **2001**, *18*, 859–866.

(12) Cameron, D. W.; Heath-Chiozzi, M.; Danner, S.; Cohen, C.; Kravcik, S.; Maurath, C.; Leonard, J. Randomised placebo-controlled trial of ritonavir in advanced HIV-1 disease. *Lancet* **1998**, *351*, 543–549.

(13) Markowitz, M.; Saag, M.; Powderly, W. G.; Hurley, A. M.; Hsu, A.; Valdes, J. M.; Ho, D. D. A preliminary study of ritonavir, an inhibitor of HIV-1 protease, to treat HIV-1 infection. *N. Engl. J. Med.* **1995**, *333*, 1534–1540.

(14) Zhang, Q.; Mei, X.-F. Polymorph transformation of solid drugs. *Acta Pharm. Sin. B* **2015**, *50*, 521–527.

(15) Singhal, D.; Curatolo, W. Drug polymorphism and dosage form design: a practical perspective. *Adv. Drug Delivery Rev.* **2004**, *56*, 335–347.

(16) Kitamura, M. Crystallization behavior and transformation kinetics of L-histidine polymorphs. *J. Chem. Eng. Jpn.* **1993**, *26*, 303–307.

(17) Srinivasan, K. Crystal growth of α and γ glycine polymorphs and their polymorphic phase transformations. *J. Cryst. Growth* **2008**, *311*, 156–162.

(18) Han, G.; Chow, P. S.; Tan, R. B. H. Direct comparison of α-and γ-glycine growth rates in acidic and basic solutions: New insights into glycine polymorphism. *Cryst. Growth Des.* **2012**, *12*, 2213–2220.

(19) Li, L.; Lechuga-Ballesteros, D.; Szkudlarek, B. A.; Rodríguez-Hornedo, N. The effect of additives on glycine crystal growth kinetics. *J. Colloid Interface Sci.* **1994**, *168*, 8–14.

(20) Polat, S.; Sayan, P. Kinetic analysis and polymorphic phase transformation of glycine in the presence of lauric acid. *J. Cryst. Growth* **2018**, *481*, 71–79.

(21) Losev, E. A.; Mikhailenko, M. A.; Achkasov, A. F.; Boldyreva, E. V. The effect of carboxylic acids on glycine polymorphism, salt and co-crystal formation. A comparison of different crystallisation techniques. *New J. Chem.* **2013**, *37*, 1973–1981.

(22) Devi, K. R.; Srinivasan, K. A novel approach to understand the nucleation kinetics of α and γ polymorphs of glycine from aqueous solution in the presence of a selective additive through charge compensation mechanism. *CrystEngComm* **2014**, *16*, 707–722.

(23) Kaptay, G. On the size and shape dependence of the solubility of nano-particles in solutions. *Int. J. Pharm.* **2012**, *430*, 253–257.

(24) Singh, A. K. *Engineered nanoparticles: structure, properties and mechanisms of toxicity*; Academic Press 2015.

(25) Doki, N.; Seki, H.; Takano, K.; Asatani, H.; Yokota, M.; Kubota, N. Process control of seeded batch cooling crystallization of the metastable α-form glycine using an in-situ ATR-FTIR spectrometer and an in-situ FBRM particle counter. *Cryst. Growth Des.* **2004**, *4*, 949–953.

(26) Mou, M.; Jiang, M. Fast Continuous Non-Seeded Cooling Crystallization of Glycine in Slug Flow: Pure α-Form Crystals with Narrow Size Distribution. *J. Pharm. Innovation* **2020**, *15*, 281–294.

(27) Azhagan, S. A. C.; Kathiravan, V. S.; Sathiya Priya, N. Crystallization, habit modification and control of nucleation of glycine polymorphs from aqueous solutions doped with magnesium sulfate impurity. *Mater. Sci.* **2018**, *36*, 483–493.

(28) Garside, J.; Davey, R. *From molecules to crystallizers: An Introduction to crystallization*; Oxford University Press 2000.

(29) Mullin, J.W. *Crystallization*, Elsevier 2001, DOI: 10.1016/B978-075064833-2/50009-7.

(30) Ely, D. R.; García, R. E.; Thommes, M. Ostwald−Freundlich diffusion-limited dissolution kinetics of nanoparticles. *Powder Technol.* **2014**, *257*, 120–123.

(31) Yang, X.; Wang, X.; Ching, C. B. Solubility of Form α and Form γ of Glycine in Aqueous Solutions. *J. Chem. Eng. Data* **2008**, *53*, 1133–1137.

(32) Igarashi, K.; Sasaki, Y.; Azuma, M.; Noda, H.; Ooshima, H. Control of Polymorphs on the Crystallization of Glycine Using a WWDJ Batch Crystallizer. *Eng. Life Sci.* **2003**, *3*, 159–163.